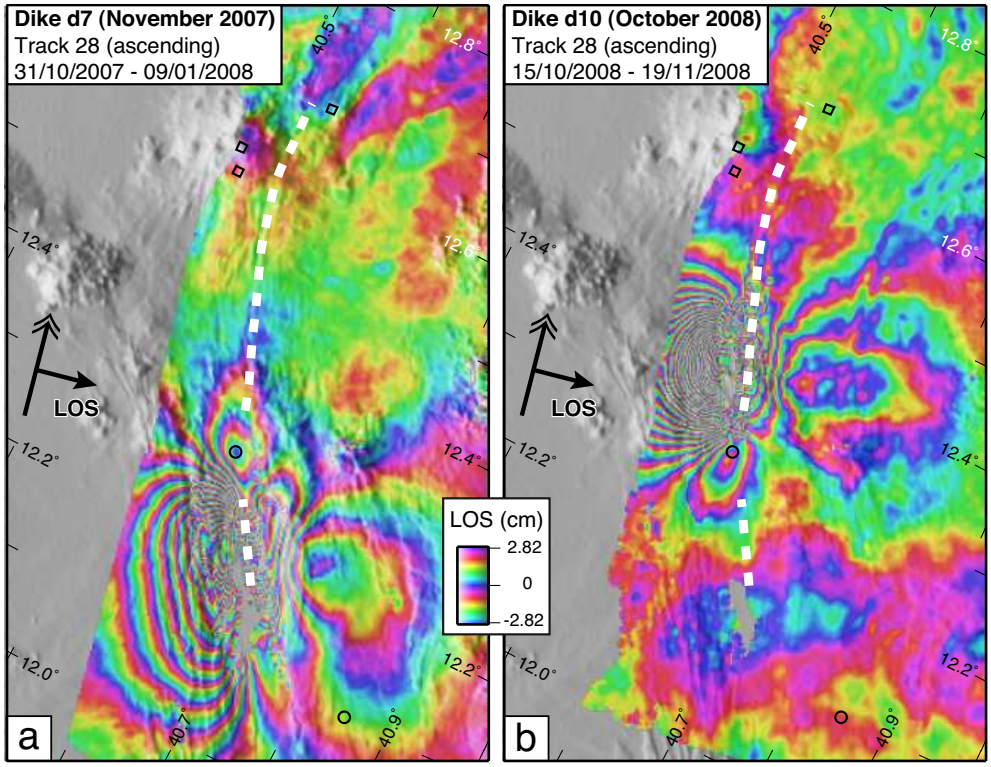

Figure S-1. Interferograms imaging the dike intrusions of November 2007 (d7, left) and October 2008 (d10, right). These two events are the most distant from the inferred central magma reservoir lying at 12.30°N (Figure 1). A small subsidence signal at the same location as sources W2 and W3 (black circle) is caused by co-diking deflation of the suspected magma source [*Hamling et al.*, 2009; *Grandin et al.*, 2010].

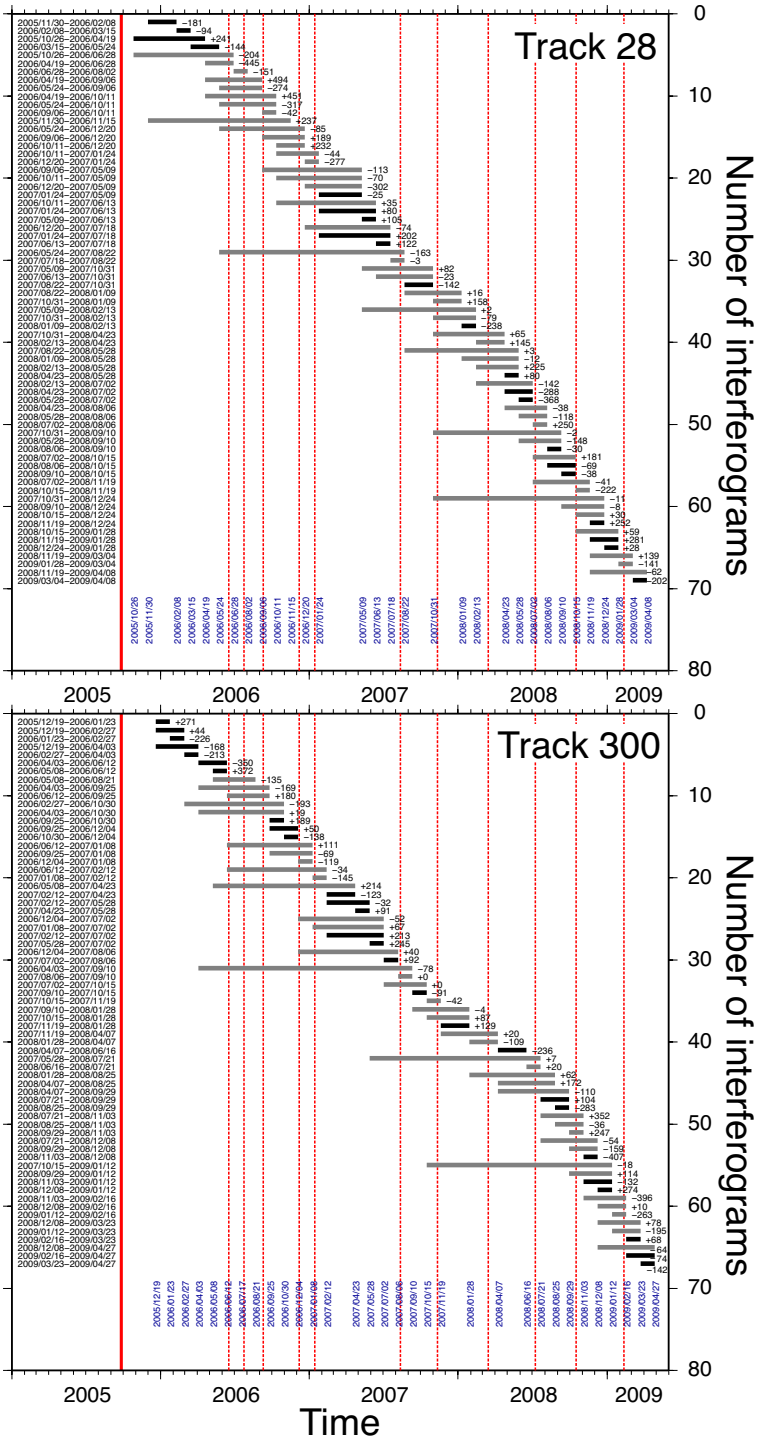

Figure S-2. InSAR data set used in this paper, for ascending tracks 28 and 300. Horizontal segments represent the time spanned by each interferogram. The black segments correspond to interferograms that image inter-diking deformation only. Grey segments represent interferograms that include deformation produced by at least one rifting event. The perpendicular baseline is indicated to the right of each segment. The dates of each SAR acquisition are shown at the bottom. The thick vertical line gives the date of the main 2005 rifting event. Thin dashed lines are for smaller subsequent rifting events.

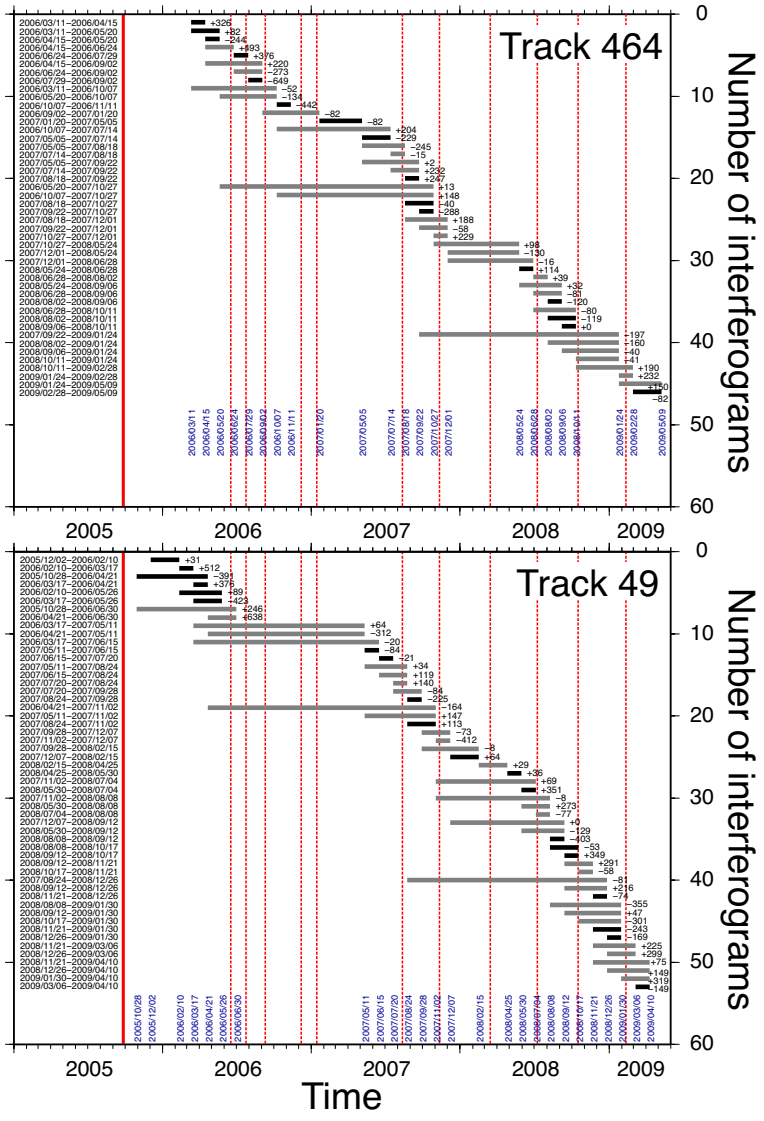

Figure S-3. Same as Figure S-2 for descending tracks 464 and 49.

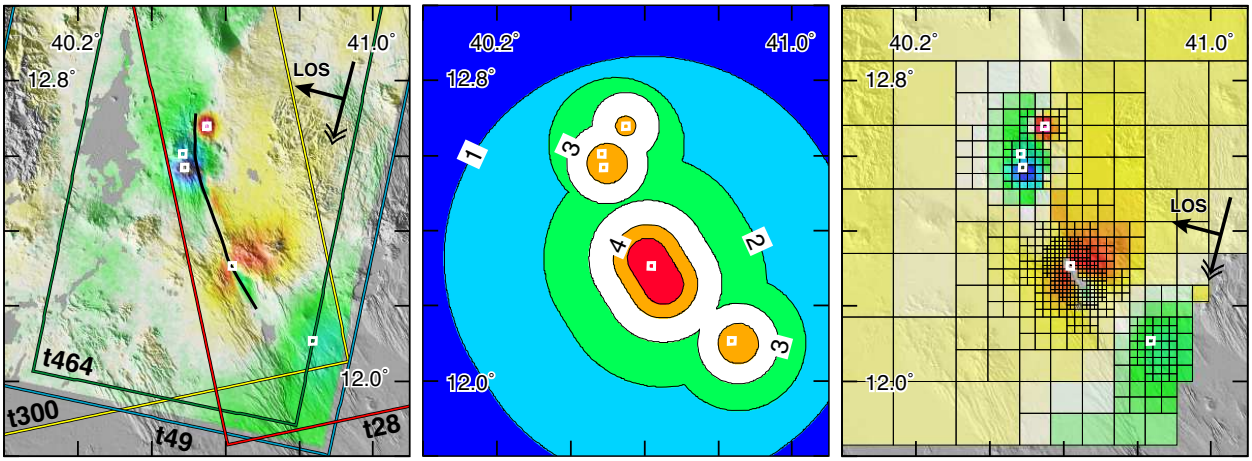

Figure S-4. Example of the result of the downsampling scheme used for elastic inversion of InSAR data. The original interferogram (left) contains hundreds of thousands of data points. Downsampling is performed by averaging InSAR measurement over successively small square areas, with the size of each square depending on the distance from inferred active geological structures (center). Surface projections of sources of transient deformation discussed in this study are shown by white squares. The surface projection of the September 2005 dike model by *Grandin et al.* [2009] is shown by a black line. The resulting set of measurements contains less than 1000 points (right). Generally, downsampled data points are not located exactly at the center of the squares shown in the figure, but rather at the isobarycenter of the data points that were averaged in each square region. The interferogram used in this example is from track 49 (descending), and spans the period from 02/12/2005 to 10/02/2006. The areas imaged by the different ENVISAT tracks used in this study are shown on the left.

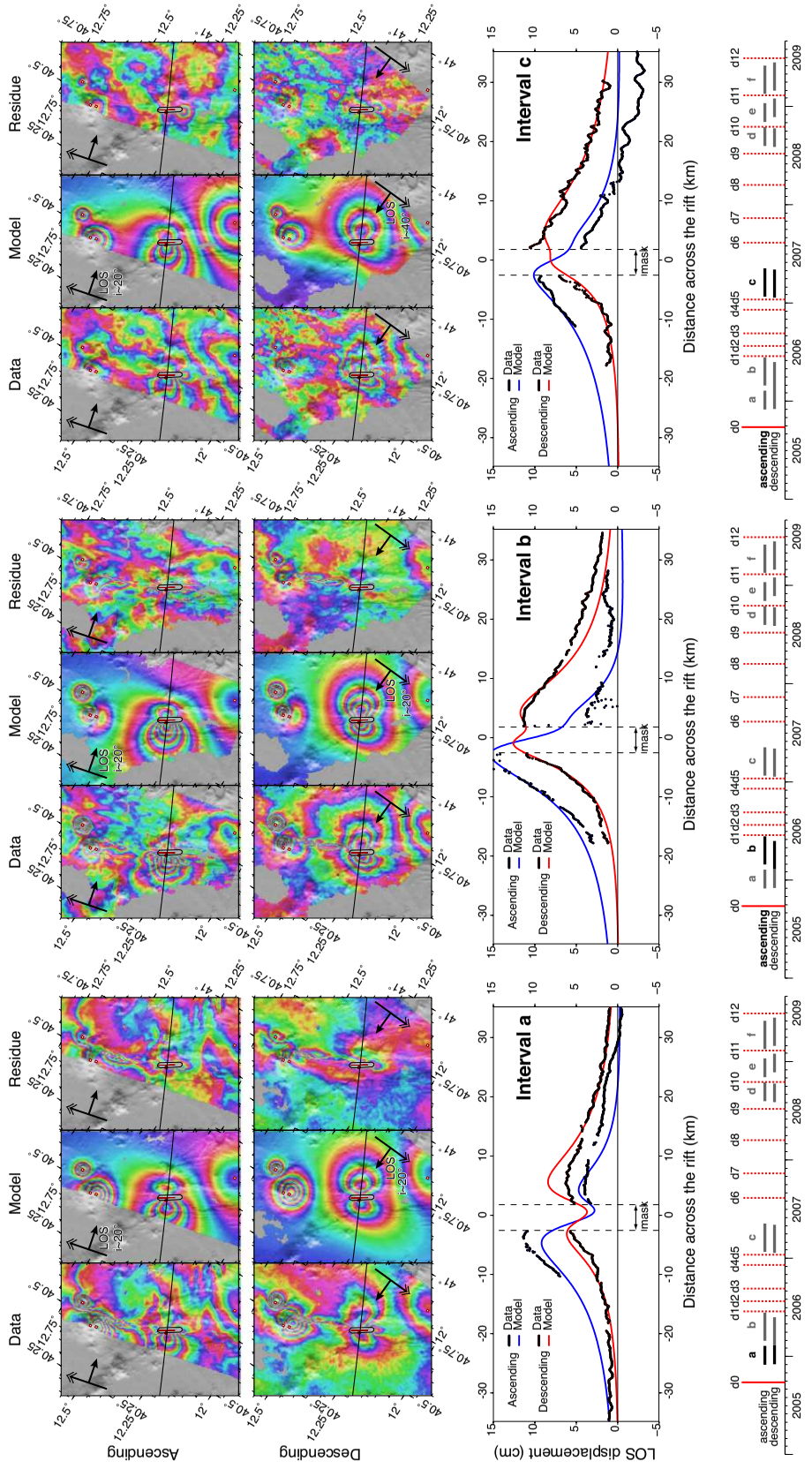

Figure S-5. Result of preliminary inversion of InSAR data for intervals a, b and c. Left: data. Middle: model. Right: residue. Top rows: ascending and descending tracks. Profiles: cross-sections in the area of deformation at the center of the Manda Hararo rift (location indicated by black line in upper panels). Bottom: dates of images used in the inversion. Double headed arrows show direction of satellite trajectory, with the approximate value of incidence angle indicated below.

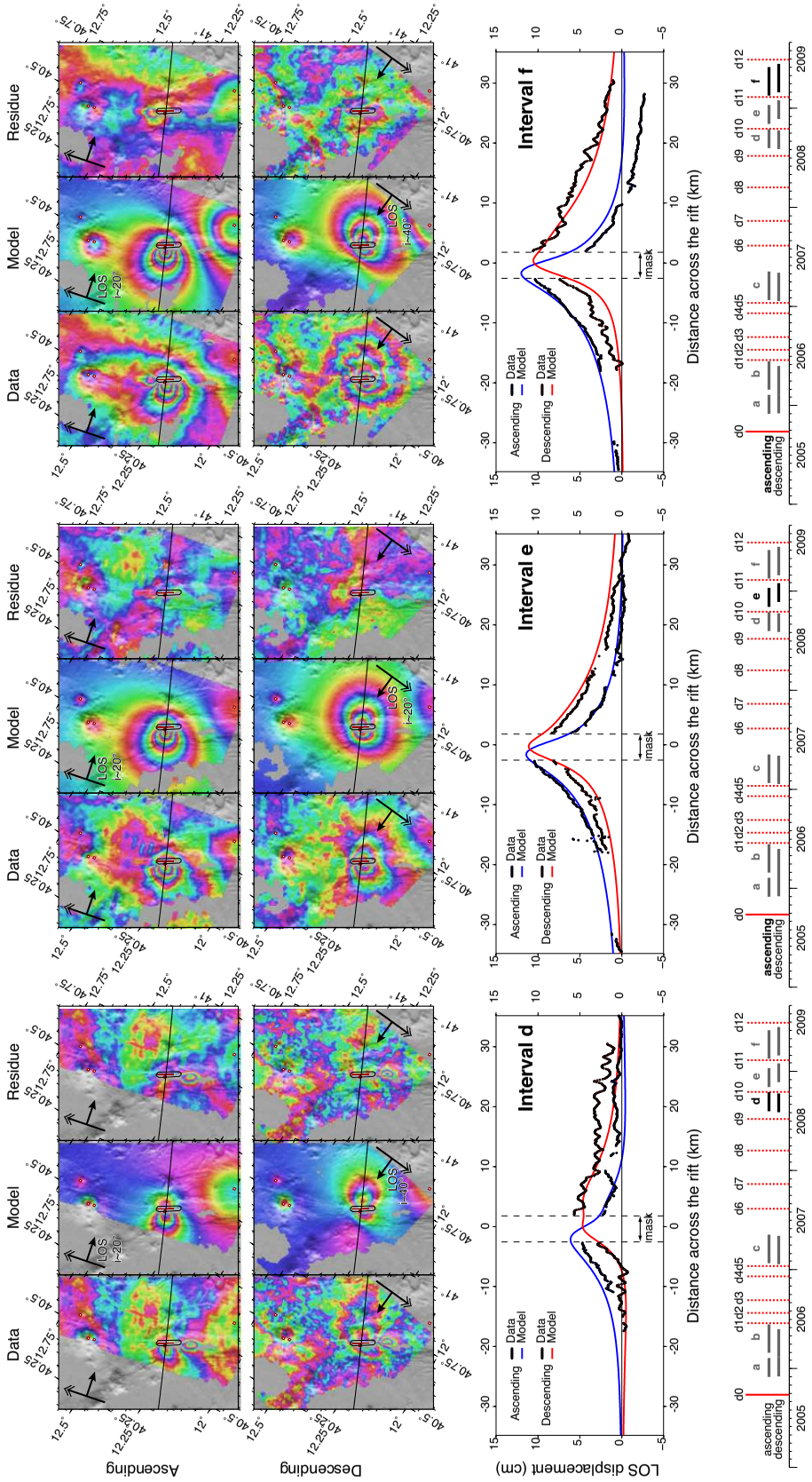

Figure S-6. Same as Figure S-5 for intervals d, e and f.

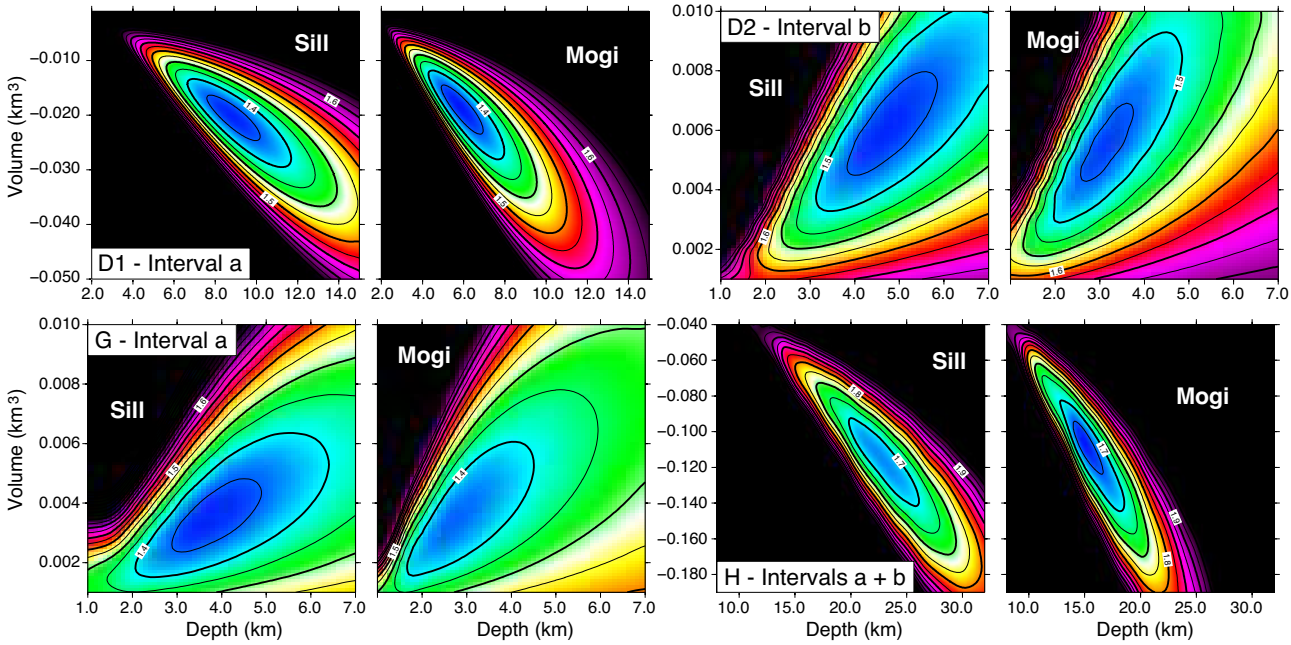

Figure S-7. RMS misfit between downsampled InSAR data and predicted LOS deformation as a function of depth and volume of sources D1 (shallow Dabbahu), D2 (deep Dabbahu), G (Gabho) and H (Hereru) in the periods that allow them to be best constrained. Contours are shown every 0.025 cm. See Figure S-5 and Table S-1 for definition of sources and time intervals. Only depth and volume of the specified source are allowed to change during each parameter exploration, and other parameters are fixed to best-fitting model deduced from non-linear inversion. Effect of changing source geometry (sill-like point-source or Mogi-source) does not change significantly the RMS misfit, while yielding different depth and volume for the best-fitting model.

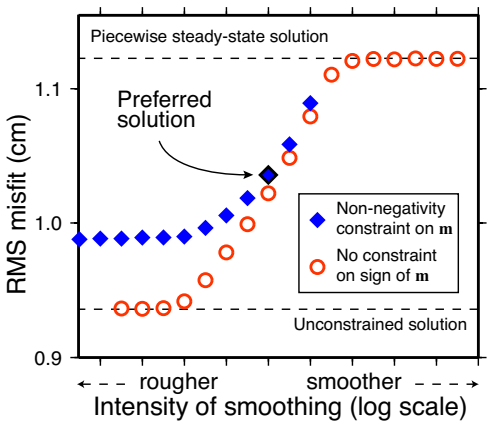

Figure S-8. Intensity of smoothing imposed in the inversion *versus* RMS misfit of the solution. A non-negativity constraint was applied on **m** (blue diamonds), but, for high degrees of smoothing, the non-negativity constraint was released to enhance the computational efficiency (red circles). The asymptote on the upper right corresponds to a steady-state solution on each interval separating two dike intrusions. The asymptote on the lower left represents the minimum RMS misfit that can be achieved with a completely unconstrained inversion.

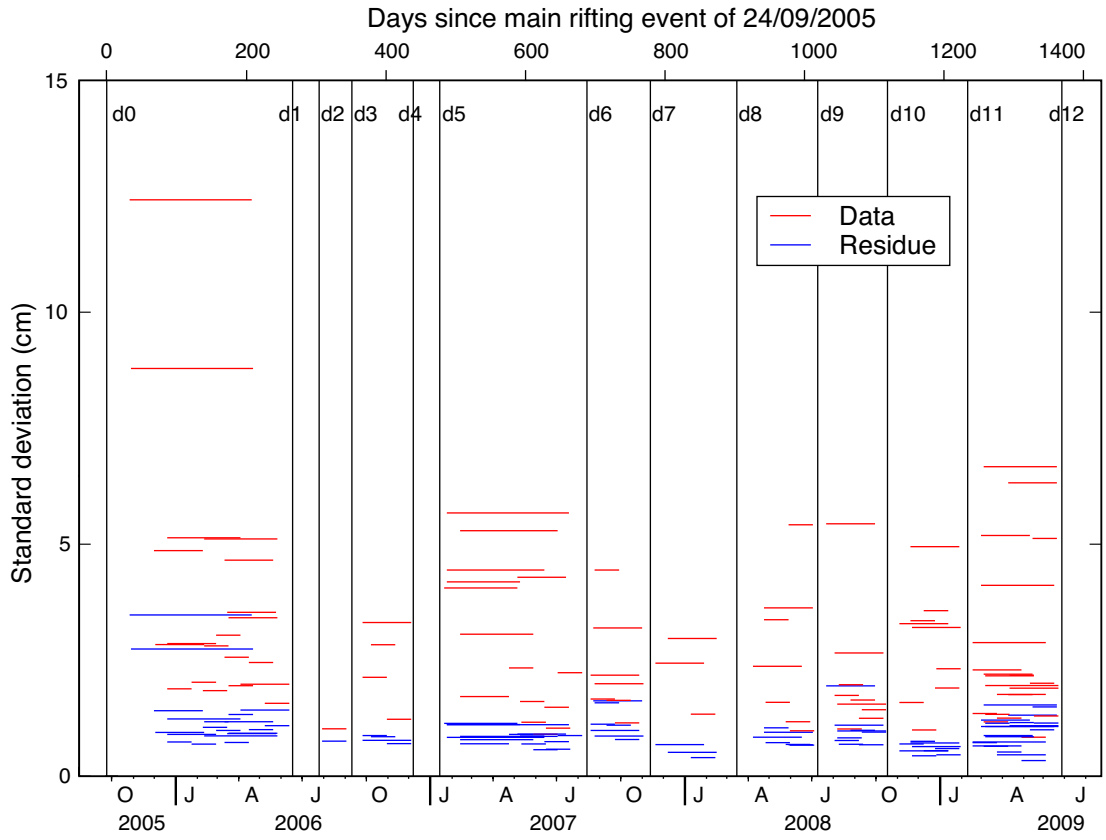

Figure S-9. Standard deviations of each downsampled interferogram (red lines) and residue after inversion (blue lines) for the preferred smoothing (Figure S-8). The length of each segment represents the time spanned by the interferogram (see also Tables S-2 and S-3).

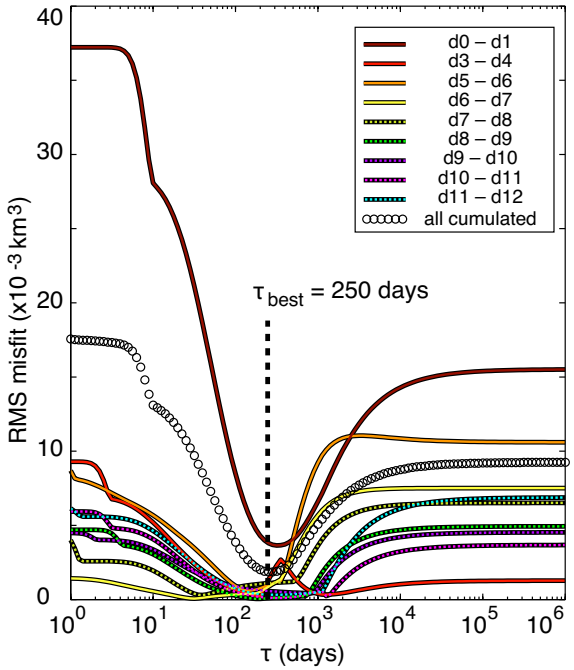

Figure S-10. RMS misfit *versus* characteristic time τ for the model of exponentially decaying activity of source W1 (see Appendix C for details). The RMS misfit between predicted activity rate of W1 and inflation rate deduced from inversion of InSAR data is calculated on each time interval as a function of τ is indicated by the colour lines (unconstrained intervals following dikes d1, d2 and d4 are not shown). A minimum RMS is found for $\tau_{best} \sim 250$ days (black dashed line).

Table 1. Geometric features of the dislocation elements (D1, D2, G and W1) and Mogi sources (W2, W3 and H) used in the elastic time-series inversion.

Element	Longitude[a] (°N)	Latitude[a] (°N)	Depth[a] (km)	Width[b] (km)	Length (km)	Strike (°N)	Dip (°N)
D1	40.477	12.575	8.8	1.0	1.0	0.0	0.0
D2	40.469	12.600	4.9	1.0	1.0	0.0	0.0
G	40.540	12.681	3.8	1.0	1.0	0.0	0.0
W1	40.629	12.306	4.0	6.0	8.0	150.0	90.0
W2	40.614	12.302	4.0	n/d	n/d	n/d	n/d
W3	40.614	12.302	25.0	n/d	n/d	n/d	n/d
H	40.850	12.099	17.0	n/d	n/d	n/d	n/d

a: location of the middle of the top of the dislocation.
b: width of dislocation along dip.
n/d: not defined.

Table S-1. Dates of acquisitions of master (T*A) and slave (T*B) SAR images used in the preliminary inversion of InSAR data for time intervals a to f (Figures S-5 and S-6), and average inflation rate for the three inflation modes at Wal'is (see Table 1 for details of the geometry of sources W1, W2 and W3).

Interval	Ascending track	T^A_{asc}	T^B_{asc}	Descending track	T^A_{desc}	T^A_{desc}	W1 ($\times 10^{-2}$ km^3/month)	W2 ($\times 10^{-2}$ km^3/month)	W3 ($\times 10^{-2}$ km^3/month)
a	28	2005-11-30	2006-02-08	49	2005-12-01	2006-02-10	1.5	0.13	3.3
b	300	2006-02-27	2006-06-12	49	2006-02-10	2006-05-26	1.2	0.26	2.1
c	28	2007-01-24	2007-05-09	464	2007-01-20	2007-05-05	0.6	0.14	3.1
d	28	2008-08-06	2008-10-15	464	2008-08-02	2008-10-11	0.7	0.17	0.2
e	300	2008-11-03	2009-01-12	49	2008-11-21	2009-01-30	0.6	0.26	3.5
f	300	2009-02-16	2009-06-01	464	2009-02-28	2009-06-13	0.5	0.20	2.4

Table S-2. Standard deviation of input data and residues for the time-series inversion.

Interferogram	Number of points	Standard deviation of data vector	Standard deviation of residue vector
20051130-20060208	505	4.860	1.411
20060208-20060315	508	1.842	1.053
20051026-20060419	505	12.422	3.476
20060315-20060524	508	3.530	0.915
20051219-20060123	533	1.882	0.734
20051219-20060227	534	2.857	0.897
20060123-20060227	534	2.025	0.688
20051219-20060403	529	5.139	1.234
20060227-20060403	533	3.036	0.985
20060403-20060612	512	1.980	1.425
20060508-20060612	532	1.569	1.086
20060311-20060415	488	2.564	0.727
20060311-20060520	490	4.656	1.173
20060415-20060520	493	2.449	1.002
20051201-20060210	563	2.837	0.940
20060210-20060317	488	2.807	1.171
20051028-20060421	516	8.788	2.742
20060317-20060421	505	1.950	1.330
20060210-20060526	528	5.112	0.867
20060317-20060526	484	3.415	0.923
Total interval d0-d1	10288	4.252	1.402
20060729-20060902	480	1.018	0.752
Total interval d2-d3	480	1.018	0.752
20060925-20061030	508	2.132	0.874
20060925-20061204	533	3.310	0.772
20061030-20061204	509	1.224	0.699
20061007-20061111	506	2.830	0.848
Total interval d3-d4	2056	2.505	0.801
20070124-20070509	499	4.187	1.111
20070124-20070613	497	4.441	0.836
20070509-20070613	509	1.609	0.864
20070124-20070718	491	5.673	1.110
20070613-20070718	490	1.485	0.742
20070212-20070423	533	1.713	0.696
20070212-20070528	530	3.058	0.784
20070423-20070528	533	2.333	0.901
20070212-20070702	516	5.290	0.857
20070528-20070702	533	0.902	0.568
20070702-20070806	526	2.230	0.875
20070120-20070505	477	4.057	1.138
20070505-20070714	477	4.288	0.906
20070511-20070615	562	1.160	0.694
20070615-20070720	529	1.032	0.581
Total interval d5-d6	7702	3.071	0.856
20070822-20071031	493	3.196	1.624
20070910-20071015	532	1.635	1.096
20070818-20070922	476	1.661	1.119
20070818-20071027	477	2.176	0.984
20070922-20071027	485	1.147	0.791
20070824-20070928	528	4.444	1.581
20070824-20071102	529	1.992	0.863
Total interval d6-d7	3520	2.122	1.194

Table S-3. Standard deviation of input data and residues for the time-series inversion (continued).

Interferogram	Number of points	Standard deviation of data vector	Standard deviation of residue vector
20080109-20080213	498	1.336	0.398
20071119-20080128	534	2.434	0.680
20071207-20080215	535	2.965	0.512
Total interval d7-d8	1567	1.813	0.545
20080423-20080528	505	3.372	1.041
20080423-20080702	497	3.626	0.946
20080528-20080702	495	5.416	0.677
20080407-20080616	531	2.366	0.839
20080524-20080628	486	1.171	0.682
20080425-20080530	536	1.591	0.722
20080530-20080704	535	0.976	0.667
Total interval d8-d9	3585	2.832	0.808
20080806-20080910	492	1.015	0.825
20080806-20081015	486	1.552	0.975
20080910-20081015	487	1.431	0.948
20080721-20080929	529	5.438	1.944
20080825-20080929	532	1.640	0.987
20080802-20080906	479	1.739	0.769
20080802-20081011	476	2.654	1.096
20080906-20081011	477	1.246	0.675
20080808-20080912	526	1.970	0.685
Total interval d9-d10	4484	2.163	1.064
20081119-20081224	490	3.350	0.751
20081119-20090128	487	4.946	0.713
20081224-20090128	494	1.899	0.595
20081103-20081208	521	1.588	0.694
20081103-20090112	521	3.286	0.545
20081208-20090112	530	3.565	0.548
20081121-20081226	533	0.993	0.438
20081121-20090130	528	3.204	0.637
20081226-20090130	536	2.316	0.460
Total interval d10-d11	4640	2.291	0.604
20090304-20090408	499	1.169	0.643
20090304-20090513	500	2.198	0.875
20090408-20090513	500	1.758	0.862
20090304-20090617	497	6.668	1.533
20090408-20090617	500	6.323	1.313
20090513-20090617	499	5.123	1.493
20090216-20090323	531	1.351	0.722
20090216-20090427	532	2.289	0.649
20090323-20090427	531	1.249	0.521
20090216-20090601	532	2.880	0.737
20090323-20090601	533	1.760	0.459
20090427-20090601	532	0.840	0.337
20090228-20090509	481	5.187	1.206
20090228-20090613	478	4.111	1.070
20090509-20090613	483	2.001	0.997
20090306-20090410	533	1.333	1.141
20090306-20090515	536	2.162	0.850
20090410-20090515	533	2.176	1.153
20090306-20090619	536	1.951	1.070
20090410-20090619	522	1.896	1.088
20090515-20090619	535	1.296	1.145
Total interval d11-d12	10823	2.827	0.993
Total all intervals	49145	3.339	1.036